A RHOMBIC PATCH MONOPOLE ANTENNA WITH MODIFIED MINKOWSKI FRACTAL GEOMETRY FOR UMTS, WLAN, AND MOBILE WIMAX APPLICATION

C. Mahatthanajatuphat, S. Saleekaw, and P. Akkaraekthalin

Faculty of Engineering
King Mongkut's University of Technology North Bangkok
Bangkok 10800, Thailand

M. Krairiksh

Faculty of Engineering
King Mongkut's Institute of Technology Ladkrabang
Bangkok 10520, Thailand

Abstract—This paper presents a rhombic patch monopole antenna applied with a technique of fractal geometry. The antenna has multiband operation in which the generator model, which is an initial model to create a fractal rhombic patch monopole, is inserted at each center side of a rhombic patch monopole antenna. Especially, a modified ground plane has been employed to improve input impedance bandwidth and high frequency radiation performance. The proposed antenna is designed and implemented to effectively support personal communication system (PCS 1.85–1.99 GHz), universal mobile telecommunication system (UMTS 1.92–2.17 GHz), wireless local area network (WLAN), which usually operate in the 2.4 GHz (2.4–2.484 GHz) and 5.2/5.8 GHz (5.15–5.35 GHz/5.725–5.825 GHz) bands, mobile worldwide interoperability for microwave access (Mobile WiMAX), and WiMAX, which operate in the 2.3/2.5 GHz (2.305–2.360 GHz/2.5–2.69 GHz) and 5.5 GHz (5.25–5.85 GHz) bands. The radiation patterns of the proposed antennas are similar to an omnidirectional radiation pattern. The properties of the antenna such as return losses, radiation patterns and gain are determined via numerical simulation and measurement.

Corresponding author: C. Mahatthanajatuphat (cmp@kmutnb.ac.th).

1. INTRODUCTION

Nowadays, wireless communication systems are becoming increasingly popular. There have been ever growing demands for antenna designs that possess the following highly desirable attributes: compact size, low profile, multi-band [1–3], wide bandwidth [4–12], etc. There are varieties of approaches that have been developed over the years, which can be utilized to achieve one or more of these design objectives. Recently, the possibility of developing antenna design objective has been improved due to the use of fractal concept. The term of the fractal geometries was originally coined by Mandelbrot [13] to describe a family of complex shapes that have self-similarity or self-affinity in their geometrical structures.

In literature reviews, we have found advantages of the fractal geometries, which support the attributes of compact size, and multiband frequency operations. Recently, the antenna design for a superior characteristic of compact size by using the fractal technique has been known as Koch monopole antenna [14]. This fractal antenna was created by iterating the initial triangle pulse through a monopole antenna. Next, a miniaturization of loop antenna using the fractal technique is known as Minkowski square loop antenna [15]. The fractal antenna was created by using the initial square pulse (SP) to iterate at each side of the loop. The extended version of miniaturization square loop antenna was found in [16], which was created by using the generator for 3/2 curve fractal to increase the electrical lengths in a fit small area. Recently, a novel microstrip patch antenna using Minkowski fractal geometry was evaluated by [17] and the new antenna with Koch shaped fractal defects on the patch surface was presented in [18].

Also, the fractal geometries still have the attributes of multiband. The Sierpinski gasket monopole antenna in [19] was introduced by Puente. This popular antenna used the self-similarity properties of the fractal shape to translate into its electromagnetic behavior. The classic Sierpinski gasket generated by Pascal triangle was introduced in [20]. However, other antennas, which have the characteristics of multiband created by fractal geometries, are following: multiple ring monopole antennas [21], coplanar waveguide (CPW) fed circular fractal slot antenna [22], and a tri-band printed antenna based on a Sierpinski gasket [23].

In this paper, we use the attributes of compact size and multiband in fractal properties applied for a rhombic patch monopole antenna, which is created by modifying the technique of Minkowski fractal concept designed for the reduction of antenna size. Additionally,

the modified ground plane on the bottom layer furthermore improves the high frequency performances, including the impedance matching bandwidth and radiation characteristics. However, the proposed antenna can be tuned to perfectly operates in the following bands of personal communication system (PCS 1.85–1.99 GHz), universal mobile telecommunication system (UMTS 1.92–2.17 GHz), wireless local area networks (WLAN 2.45 GHz/5.2 GHz/5.8 GHz), mobile worldwide interoperability for microwave access (Mobile WiMAX 2.3 GHz/2.5 GHz), and WiMAX 5.5 GHz. The various parameters of the proposed antenna on the top and bottom metallic layers will be investigated by simulation using the full wave method of moments (MoM) software package from IE3D. The experiments of the fabricated antenna prototype have also been performed. Especially, the radiation patterns of the proposed antenna will be evaluated and observed.

The organization of this paper is as follows. In Section 2, a brief explanation on the fractal rhombic monopole antenna design will be given. Then, the antenna parameters will be studied in Section 3. After that, simulation and measured properties of the proposed antenna will be discussed in Section 4. Finally, the results are discussed in Section 5.

2. ANTENNA DESIGN

In this section, the radiating patch of antenna is created by generating the initial generator model at each side of a rhombic patch, as shown in Fig. 1, and then it has been modified by fulfilling with metal to some eroded edges of Minkowski fractal rhombic patch with the second iteration that is shown in the shaded areas of Fig. 2. The altitude of initial generator model as depicted in Fig. 1 alters with W_p. Generally, W_p is smaller than $W_s/3$ and the iteration factor is [24]

$$\eta = \frac{W_p}{W_s/3}; \qquad 0 < \eta < 1 \tag{1}$$
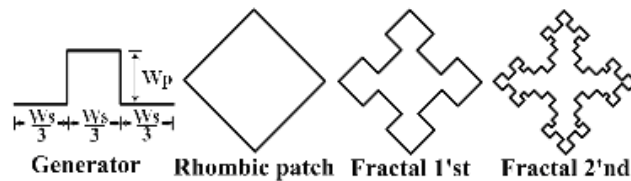
Figure 1. The initial generator model for creating fractal rhombic patch.

The configuration of the proposed antenna, as illustrated in Fig. 2, is a rhombic patch monopole antenna with a modified Minkowski fractal geometry at the second iteration and a modified ground plane. The antenna consists of a radiating patch with a patch width W_s, which is fed by a microstrip line to match impedance $50\,\Omega$ with a strip width W_f on the top layer, and a modified ground plane of the antenna placed beneath the radiating patch on the bottom layer to improve the impedance bandwidth and radiation performances at high frequency. The dimensions of the modified ground plane include the widths W_g, W_{gt}, W_{gf} and the lengths L_g, L_{gt}, L_{gf}. The small gap between radiating patch and modified ground plane is denoted as g.

In this paper, we exploit the iteration factor $\eta = 0.66$ and fabricate the proposed antenna on an economical FR4 dielectric with a thickness of $1.6\,\text{mm}$ (h), relative permittivity of 4.1 (ε_r), and loss tangent of 0.019. The total dimensions of the antenna are $59\,\text{mm} \times 90\,\text{mm} \times 1.6\,\text{mm}$. A $50\,\Omega$ SMA connector is used to feed the antenna at the microstrip line of radiating patch monopole antenna, in which the approximate width $W_f = 3.48\,\text{mm}$ and length $L_f = 11.55\,\text{mm}$ are fixed as shown in Fig. 2. The modified radiating
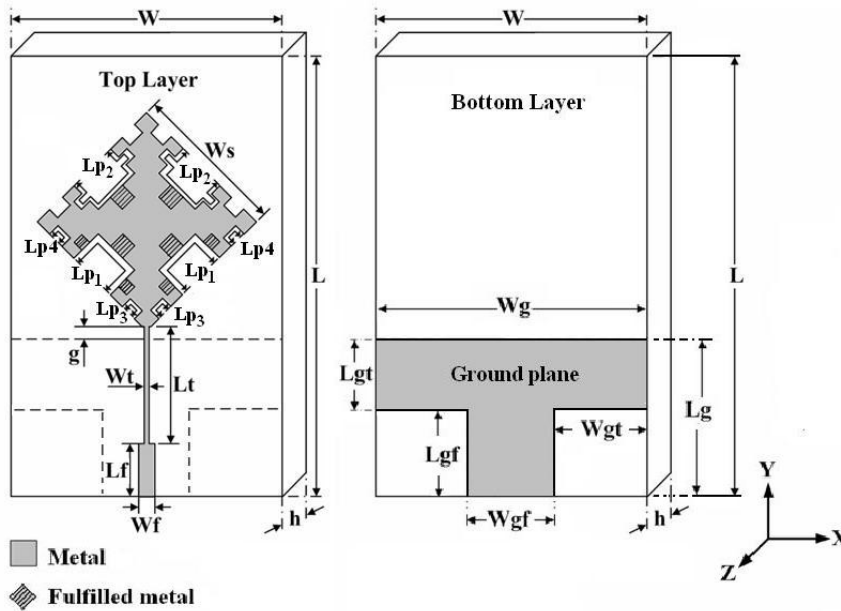

Figure 2. Schematic diagram of the rhombic patch monopole antenna with a modified Minkowski fractal geometry and a modified ground plane.

patch monopole antenna has dimensions of $33.54\,\text{mm} \times 33.54\,\text{mm}$ and is placed on the top metallic layer of the antenna to cover the operating application frequency bands of 1.9 GHz, 2.1 GHz, 2.3 GHz, 2.45 GHz, 2.5 GHz, 5.2 GHz, 5.5 GHz, and 5.8 GHz. The significant parameters, which influence the resonant frequencies of 2.13 GHz, 4.46 GHz, and 5.56 GHz, consist of L_{p1}, L_{p2}, L_{p3}, L_{p4}, g, and W_t, respectively. Due to the proposed antenna is a complicated structure to calculate by carrying out analytical technique, the 3-D full wave electromagnetic (IE3D) coded by Zeland is properly applied to powerfully analyze the characteristics of the proposed antenna including return loss, gain, current distribution, and radiation pattern. The initial parameters of the proposed antenna are following: $h = 1.6\,\text{mm}$, $W = W_g = 59\,\text{mm}$, $L = 90\,\text{mm}$, $L_g = 35.25\,\text{mm}$, $W_s = 33.54\,\text{mm}$, $L_t = 25.36\,\text{mm}$, $W_f = 3.48\,\text{mm}$, $L_f = 11.55\,\text{mm}$, $L_{gt} = 17.60\,\text{mm}$, $L_{gf} = 17.65\,\text{mm}$, $W_{gt} = 21\,\text{mm}$, and $W_{gf} = 17\,\text{mm}$. The important parameters of L_{p1}, L_{p2}, L_{p3}, L_{p4}, g, and W_t are investigated to observe the variation of the operating frequency for each band in the next section.

3. PARAMETER STUDY

This section presents the important parameters, such as L_{p1}, L_{p2}, L_{p3}, L_{p4}, g, and W_t, which influence the operating frequency bands of 2.13 GHz, 4.46 GHz, and 5.56 GHz. Then, the parameter effects of the proposed antenna on impedance bandwidth and radiation pattern are illustrated.
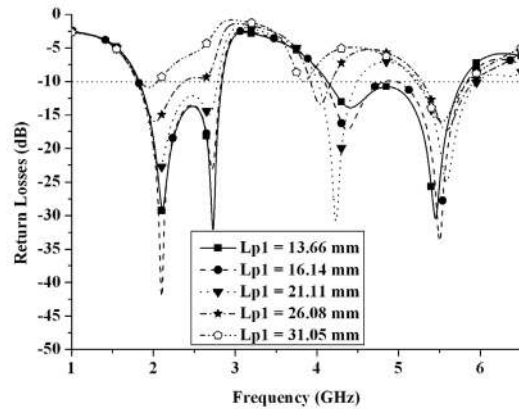
Figure 3. Simulated return losses for various L_{p1} with $L_{p2} = 36.02\,\text{mm}$, $L_{p3} = 8.69\,\text{mm}$, $L_{p4} = 8.69\,\text{mm}$, $g = 1.15\,\text{mm}$, and $W_t = 1.15\,\text{mm}$.

For this design, the antenna configuration parameters, as illustrated in Fig. 2, have been chosen to be $L_{p2} = 36.02$ mm, $L_{p3} = 8.69$ mm, $L_{p4} = 8.69$ mm, $g = 1.15$ mm, $W_t = 1.15$ mm and then the parameter L_{p1} has been varied ($L_{p1} = 13.66, 16.14, 21.11, 26.08$, and 31.05 mm). The return losses of the designed antenna are shown in Fig. 3. From the figure, the antenna has four resonant frequencies. As the L_{p1} increases, the return losses of the first and second resonant frequencies become worse and the resonant frequencies decrease, while the center frequencies of the third and fourth resonant frequencies are shifted to the left and right, respectively and the peak between the third and fourth resonant frequencies also increases. In this case, the appropriate parameter $L_{p1} = 16.14$ mm is chosen to cover the operating frequency band of 1.8–2.82 GHz and to design the configuration of the next step.
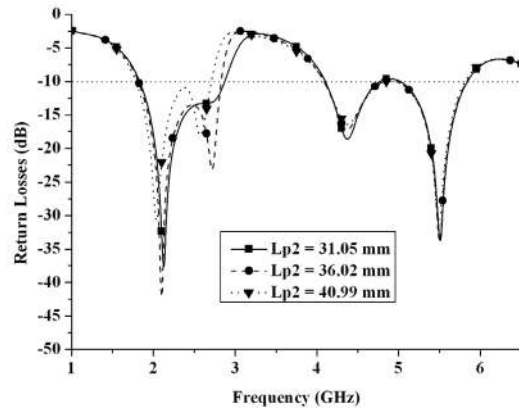
Figure 4. Simulated return losses for various L_{p2} with $L_{p1} = 16.14$ mm, $L_{p3} = 8.69$ mm, $L_{p4} = 8.69$ mm, $g = 1.15$ mm, and $W_t = 1.15$ mm.

In order to improve the bandwidth of the first and second resonant frequencies, the parameter $L_{p1} = 16.14$ mm has been selected from the previous step; $L_{p3} = 8.69$ mm, $L_{p4} = 8.69$ mm, $g = 1.15$ mm, and $W_t = 1.15$ mm are unchanged; and the parameter L_{p2} is varied to be 31.05, 36.02, and 40.99 mm. The return losses with variation of L_{p2} are depicted in Fig. 4. It can be found that the parameter L_{p2} increases from 31.05 mm to 40.99 mm, resulting in the decrease of the center frequencies of the first and second resonances. The return loss of the second resonant frequency also decreases. It can be seen that the parameter L_{p2} does not significantly afftect the third and fourth resonant frequencies. Therefore, the suitable parameter of

$L_{p2} = 36.02$ mm is preferred to cover the operating frequency range of 1.8–2.82 GHz.
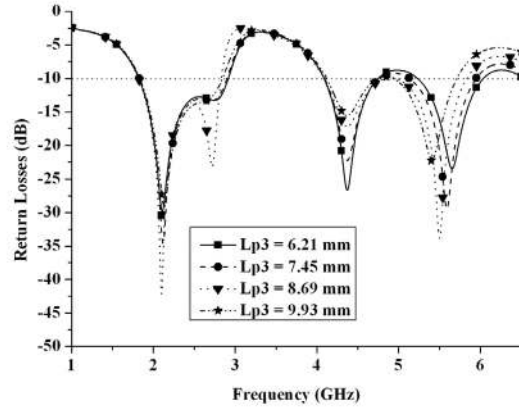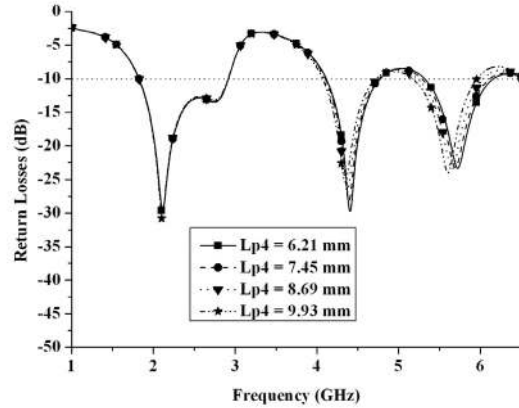

Figure 5. Simulated return losses for various L_{p3} with $L_{p1} = 16.14$ mm, $L_{p2} = 36.02$ mm, $L_{p4} = 8.69$ mm, $g = 1.15$ mm, and $W_t = 1.15$ mm.

Next, the effect of the fourth resonant frequency is investigated by varying parameter $L_{p3} = 6.21$, 7.45, 8.69, and 9.93 mm, while other parameters $L_{p1} = 16.14$ mm, $L_{p2} = 36.02$ mm, $L_{p4} = 8.69$ mm, $g = 1.15$ mm, and $W_t = 1.15$ mm are selected. The results of altering the parameter L_{p3} are depicted in Fig. 5. As the parameter L_{p3} increases, the main effect of frequency shifting is occurred at the fourth resonant frequency and the peak return loss between the third and fourth resonances slightly decreases. Also, the return losses of the first and third resonant frequencies increase. In order to cover the operating frequencies range 5.725–5.825 GHz, the appropriate parameter $L_{p3} = 6.21$ mm is selected.

However, the effects of the third and fourth resonant frequencies are still investigated by varying the parameter L_{p4} to be 6.21, 7.45, 8.69, and 9.93 mm. The previous parameters $L_{p1} = 16.14$ mm, $L_{p2} = 36.02$ mm, $L_{p3} = 6.21$ mm, $g = 1.15$ mm, and $W_t = 1.15$ mm are chosen. The alternate parameter L_{p4} causes slight change of the third and fourth resonant frequencies as shown in Fig. 6. In this figure, it can be seen that the third and fourth resonant frequencies decrease due to the parameter L_{p4} increases and the return loss of the fourth resonant frequency slightly decreases. The suitable parameter $L_{p4} = 7.45$ mm is selected to cover the operating frequency band of 5.8 GHz.

Then, the gap between the radiating patch and the modified ground plane is investigated. The significant effect on the impedance

Figure 6. Simulated return losses for various L_{p4} with $L_{p1} = 16.14$ mm, $L_{p2} = 36.02$ mm, $L_{p3} = 6.21$ mm, $g = 1.15$ mm, and $W_t = 1.15$ mm.
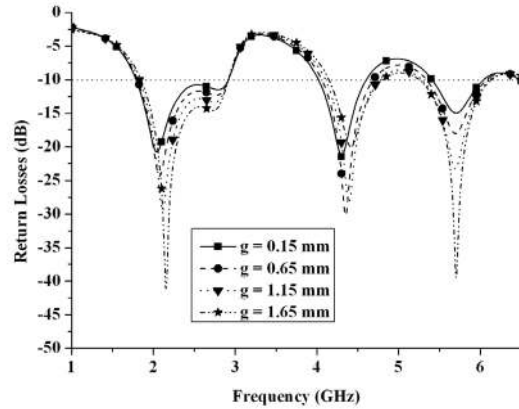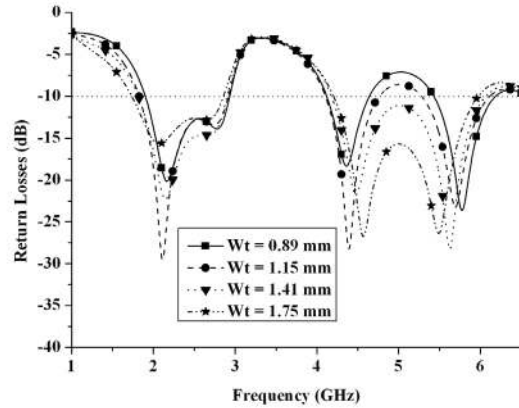

Figure 7. Simulated return losses for various g with $L_{p1} = 16.14$ mm, $L_{p2} = 36.02$ mm, $L_{p3} = 6.21$ mm, $L_{p4} = 7.45$ mm, and $W_t = 1.15$ mm.

matching of the proposed antenna, as illustrated in Fig. 7, can be clearly seen. As the gap g is increased from 0.15 to 1.65 mm, the impedance matching at all of resonant frequencies can be greatly improved. Also, the suitable gap $g = 1.15$ mm is chosen. Lastly, another significant parameter for the impedance bandwidth matching at all of resonant frequencies is W_t. The effect of the parameter W_t is investigated by varying W_t from 0.89 to 1.75 mm, as shown in Fig. 8. As W_t increases, it can be clearly observed that the return loss of

the first resonance is higher, while the peak return loss between the third and fourth resonant frequencies decreases. Therefore, in order to cover the operating frequency band of 4.15–5.95 GHz, the appropriate parameter $W_t = 1.41$ mm should be chosen.

Figure 8. Simulated return losses for various W_t with $L_{p1} = 16.14$ mm, $L_{p2} = 36.02$ mm, $L_{p3} = 6.21$ mm, $L_{p4} = 7.45$ mm, and $g = 1.15$ mm.

Additionally, another effect of the modified ground plane on the radiation characteristic will be investigated. Normally, in a low
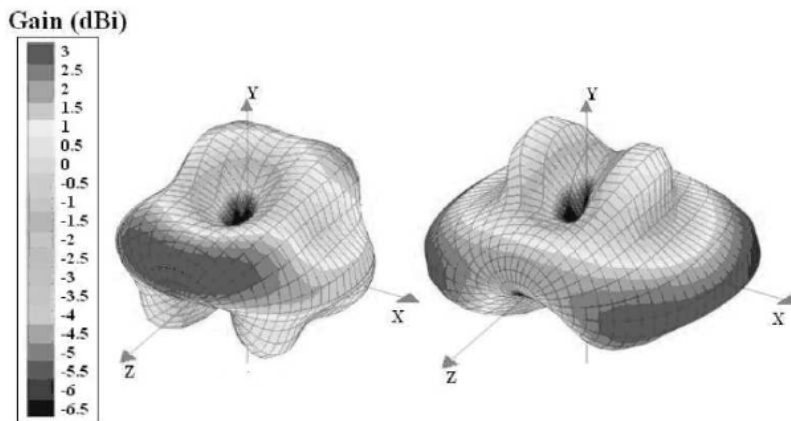
Figure 9. Simulated 3-D radiation pattern at 5.56 GHz of the modified fractal rhombic patch monopole antenna with (a) Rectangular ground plane and (b) modified ground plane.

frequency band, the radiation pattern of the proposed antenna is effectively omnidirectional, but it has usually been deteriorated in a high frequency region, i.e., at the operating frequency of 5.56 GHz. The distorted pattern at high frequency is caused by the magnetic current mainly distributed over the gap between the radiating patch and the ground plane. The traveling waves move through the gap, resulting in directional radiation patterns in the horizontal plane (xz-plane). By presenting the modified ground plane, the transverse currents on it are improved comparing with a rectangular ground plane. Therefore, at the high frequencies about 5.56 GHz, the currents on the modified ground plane are rearranged, then more power is fed into the gap between the radiating patch and the modified ground plane to radiate the waves from the gap, resulting in the propagation of an improved omnidirectional pattern. As the result, the gains in high frequency are

Table 1. Summary of parameters study of the proposed antenna with different parameters.

Parameters(mm)					
L_{p1}	L_{p2}	L_{p3}	L_{p4}	g	W_t
13.66 16.14 21.11 26.08 31.05	36.02	8.69	8.69	1.15	1.15
16.14	31.05 36.02 40.99	8.69	8.69	1.15	1.15
16.14	36.02	6.21 7.45 8.69 9.93	8.69	1.15	1.15
16.14	36.02	6.21	6.21 7.45 8.69 9.93	1.15	1.15
16.14	36.02	6.21	7.45	0.15 0.65 1.15 1.65	1.15
16.14	36.02	6.21	7.45	1.15	0.89 1.15 1.41 1.75

enhanced. Fig. 9 shows the comparison of the simulated 3-D radiation patterns between the proposed antenna with a rectangular ground plane, including the parameters of $L_{gt} = 35.25$ mm, $L_{gf} = 0$ mm, $W_{gt} = 0$ mm, and $W_{gf} = 59$ mm and with the modified ground plane, including the optimal parameters of $L_{gt} = 17.60$ mm, $L_{gf} = 17.65$ mm, $W_{gt} = 21$ mm, and $W_{gf} = 17$ mm, at 5.56 GHz. It can be seen that the radiation pattern with the modified ground plane is improved to be more omnidirectional than that with the rectangular ground plane in the horizontal plane (xz-plane).

In order to take the most advantages for the applications in wireless communication systems, the appropriate parameters, which are $L_{p1} = 16.14$ mm, $L_{p2} = 36.02$ mm, $L_{p3} = 6.21$ mm, $L_{p4} = 7.45$ mm, $g = 1.15$ mm, $W_t = 1.41$ mm, are selected for the investigation of the current distributions, radiation patterns and gain of each resonant frequency in the next section. The parameter studies of the proposed antenna are summarized in Table 1.
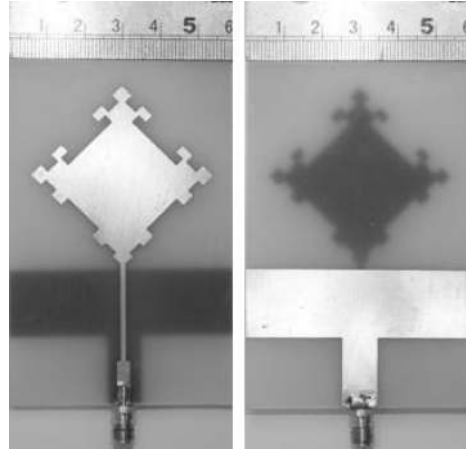

Figure 10. Photograph of the proposed antenna with appropriate values of $L_{p1} = 16.14$ mm, $L_{p2} = 36.02$ mm, $L_{p3} = 6.21$ mm, $L_{p4} = 7.45$ mm, $g = 1.15$ mm, and $W_t = 1.41$ mm.

4. EXPERIMENTAL RESULTS

From the investigation of various parameters that affect the operating frequency bands of the proposed antenna in the previous section, the appropriate parameters including $W = W_g = 59$ mm, $L = 90$ mm, $L_g = 35.25$ mm, $W_s = 33.54$ mm, $L_t = 25.36$ mm, $W_f = 3.48$ mm,

$L_f = 11.55\,\mathrm{mm}$, $L_{p1} = 16.14\,\mathrm{mm}$, $L_{p2} = 36.02\,\mathrm{mm}$, $L_{p3} = 6.21\,\mathrm{mm}$, $L_{p4} = 7.45\,\mathrm{mm}$, $g = 1.15\,\mathrm{mm}$, $W_t = 1.41\,\mathrm{mm}$, $L_{gt} = 17.60\,\mathrm{mm}$, $L_{gf} = 17.65\,\mathrm{mm}$, $W_{gt} = 21\,\mathrm{mm}$, and $W_{gf} = 17\,\mathrm{mm}$, are selected to construct the prototype antenna by etching into chemicals, as shown in Fig. 10. Fig. 11 shows simulated and measured return losses of the optimal proposed antenna. The simulated result shows three resonant frequencies at 2.13 GHz, 4.46 GHz, and 5.56 GHz, while the measured result has similarly resonant frequencies at 2.17 GHz, 4.47 GHz, and 5.6 GHz. All return loss results are summarized in Table 2.
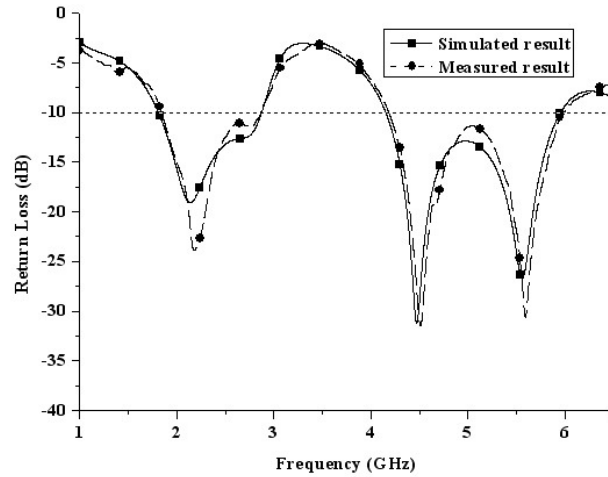

Figure 11. Simulated and measured return losses for the proposed antenna.

**Table 2.** Resonant frequency and return loss results of the proposed antenna.

Operating frequency Band		First	Second	Third
Resonant frequency (GHz)	Simulated results	2.13	4.46	5.56
	Measured results	2.17	4.47	5.6
Return loss (dB)	Simulated results	−19	−32	−27
	Measured results	−24	−32	−32

Both simulated and measured results are in quite good agreement, which cover PCS, UMTS, WLAN, Mobile WiMAX bands. Therefore, the proposed antenna can be applied for PCS 1900, UMTS, WLAN, and Mobile WiMAX system.

The excited surface current distributions, determined by the IE3D simulation, on the radiating modified fractal rhombic patch of the proposed antenna at 2.13 GHz, 4.46 GHz, and 5.56 GHz are illustrated in Fig. 12. For the excitation at 2.13 GHz as shown in Fig. 12(a), a larger surface current distribution is observed from the radiating patch along the length L_a. Also, it can be clearly seen that the parameters L_{p1}, L_{p2}, and L_{p4}, as mentioned in the previous section, relate to the length L_a and influence with the resonant frequency 2.13 GHz. At this frequency, the length L_a is about 98.139 mm or 0.696 λ_o.


(a)

(b)

(c)
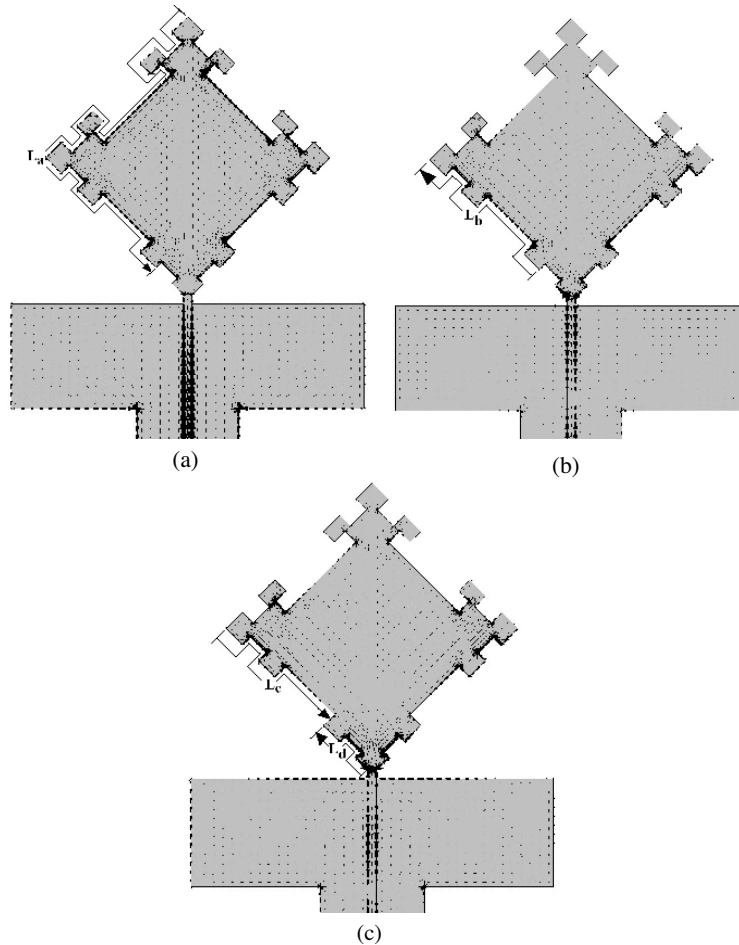
Figure 12. Simulated IE3D results of the surface current distributions on the radiating modified fractal rhombic patch of the proposed antenna at (a) 2.13 GHz, (b) 4.46 GHz, and (c) 5.56 GHz.

(a)

(b)
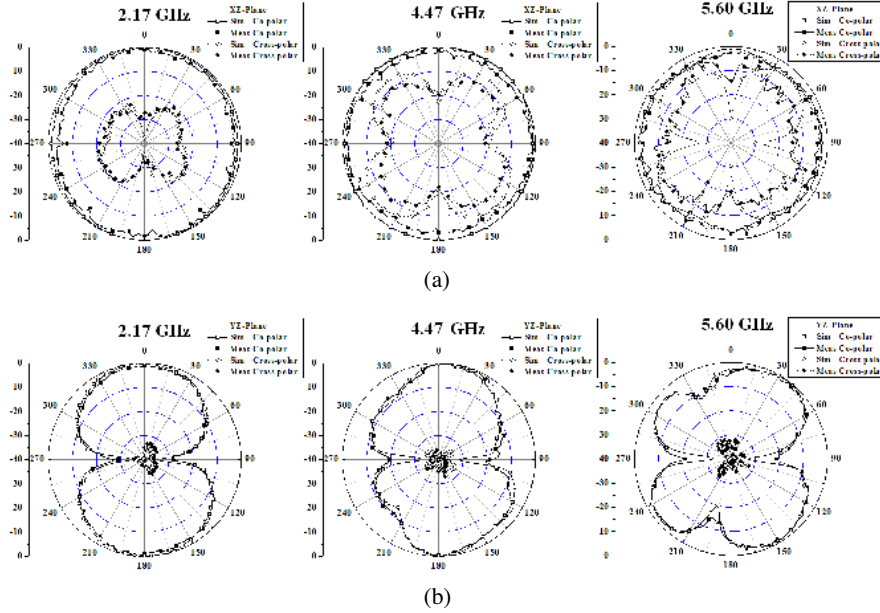
Figure 13. Measured radiation patterns of the proposed antenna with $L_{p1} = 16.14\,\text{mm}$, $L_{p2} = 36.02\,\text{mm}$, $L_{p3} = 6.21\,\text{mm}$, $L_{p4} = 7.45\,\text{mm}$, $g = 1.15\,\text{mm}$, and $W_t = 1.41\,\text{mm}$ at 2.17 GHz, 4.47 GHz, and 5.60 GHz for (a) X-Z plane and (b) Y-Z plane.

Also, Fig. 12(b) illustrates that it has a larger current distribution on the half of lowest path of radiating patch. It is obvious that the currents flow through the eroded edges, which depend on the parameter L_{p1} and L_{p4}, as mentioned in Section 3, along the length L_b to radiate E-pattern at 4.46 GHz. The L_b is about 34.783 mm or $0.517\lambda_o$. Fig. 12(c) depicts that a lager surface current distribution flows down passing the eroded edges, which depends on the parameter L_{p1} and L_{p4}, along the length L_c about 28.52 mm or $0.528\lambda_o$, while another larger surface current distribution flows up passing the eroded edges, which depend on the parameter L_{p3}, along the length L_d about 12.42 mm or $0.230\lambda_o$. It reveals that both opposite currents must disturb some parts of the radiation pattern at 5.56 GHz, resulting in the non-perfectly omnidirectional radiation pattern.

Figures 13(a) and (b) show the simulated and measured radiation patterns in X-Z and Y-Z planes for the proposed antenna at 2.17 GHz, 4.47 GHz, and 5.6 GHz. It can be clearly seen that the results are in good agreement. The simulated and measured radiation patterns of
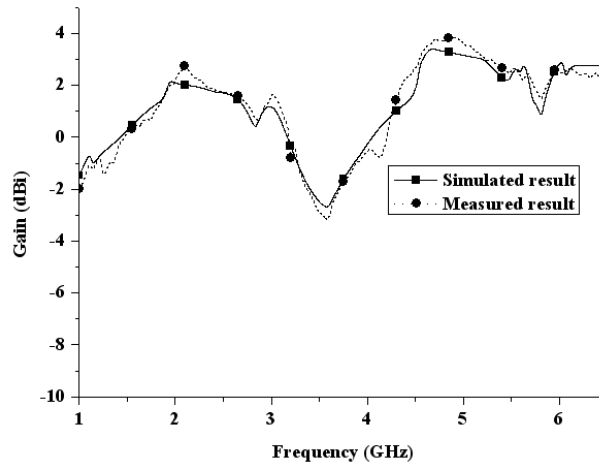
Figure 14. Simulated and measured gains of the proposed antenna.

all operating frequency bands, as shown in Fig. 13(a), are similar to an omnidirectional radiation. It can be noticed that the magnitude of cross polarization in X-Z plane increases with operating frequencies at 2.17 GHz, 4.47 GHz, and 5.6 GHz. In Fig. 13(b), the maximum gains of radiation patterns in Y-Z plane approximately occurr at 0 and 180 degrees, at the resonant frequencies of 2.17 GHz and 4.47 GHz. For the resonant frequency of 5.6 GHz, the maximum gain of radiation pattern in Y-Z plane approximately occurrs at 30 and 150 degrees due to the disturbance between the current flow along the lengths L_c and L_d. However, at the resonant frequency of 5.6 GHz, the proposed antenna can radiate the pattern similar to an omnidirectional.

Figure 14 depicts that the peaks of simulated gain of each operating frequency at 2.13 GHz, 4.46 GHz, and 5.56 GHz are approximately 2, 3, and 2 dBi, respectively, and the peaks of measured gain at each frequency of 2.17 GHz, 4.47 GHz, and 5.6 GHz are approximately 2, 3, and 2 dBi, respectively. However, varied parameters, i.e., $L_{p1}, L_{p2}, L_{p3}, L_{p4}, g,$ and W_t, slightly affect the antenna gain. As the results, the average gain of the simulated and measured results is about 2 dBi at the resonant frequency.

5. CONCLUSION

In this paper, the modified fractal rhombic patch monopole antenna has been investigated. The configuration parameters of the proposed antenna have been tuned to enhance the impedance

bandwidth for operating in any wireless communication system band. From measured results, the proposed antenna is surely appropriate to apply for wireless communication systems including PCS 1900 (1.85–1.99 GHz), UMTS (1.92–2.17 GHz), WLAN (2.40–2.48 GHz/5.15–5.35 GHz/5.725–5.825 GHz), Mobile WiMAX (2.3–2.36 GHz/2.5–2.69 GHz), and WiMAX (5.25–5.85 GHz). In addition, the proposed antenna can radiate omnidirectional patterns at all of the operating frequency bands suitable for using in wireless communication applications, which is a key advantage of the fractal antennas over the conventional multiband antennas.

ACKNOWLEDGMENT

REFERENCES

1. Song, Y., Y.-C. Jiao, G. Zhao, and F.-S. Zhang, "Multiband CPW-FED triangle-shaped monopole antenna for wireless applications," *Progress In Electromagnetics Research*, PIER 70, 329–336, 2007.

2. Elsadek, H. and D. M. Nashaat, "Band compact size trapezoidal PIFA antenna," *Journal of Electromagnetic Waves and Applications*, Vol. 21, No. 7, 865–876, 2007.

3. Liu, W. C. and H.-J. Liu, "Miniaturized asymmetrical CPW-FED meandered strip antenna for triple-band operation," *Journal of Electromagnetic Waves and Applications*, Vol. 21, No. 8, 1089–1097, 2007.

4. Ang, B.-K. and B.-K. Chung, "A wideband E-shaped microstrip patch antenna for 5–6 GHz wireless communications," *Progress In Electromagnetics Research*, PIER 75, 397–407, 2007.

5. Wang, F. J. and J.-S. Zhang, "Wideband cavity-backed patch antenna for PCS/IMT2000/2.4 GHz WLAN," *Progress In Electromagnetics Research*, PIER 74, 39–46, 2007.

6. Eldek, A. A., A. Z. Elsherbeni, and C. E. Smith, "Characteristics oF bow-tie slot antenna with tapered tuning stubs for wideband operation," *Progress In Electromagnetics Research*, PIER 49, 53–69, 2004.

7. Eldek, A. A., A. Z. Elsherbeni, and C. E. Smith, "Design of wideband triangle slot antennas with tuning stub," *Progress In Electromagnetics Research*, PIER 48, 233–248, 2004.

8. Khodae, G. F., J. Nourinia, and C. Ghobadi, "A practical miniaturized U-slot patch antenna with enhanced bandwidth," *Progress In Electromagnetics Research B*, Vol. 3, 47–62, 2008.

9. Danideh, A., R. Sadeghi Fakhr, and H. R. Hassani, "Wideband co-planar microstrip patch antenna," *Progress In Electromagnetics Research Letters*, Vol. 4, 81–89, 2008.

10. Abbaspour, M. and H. R. Hassani, "Wideband star-shaped microstrip patch antenna," *Progress In Electromagnetics Research Letters*, Vol. 1, 61–68, 2008.

11. Liu, Y.-T. and C.-W. Su, "Wideband omnidirectional operation monopole antenna," *Progress In Electromagnetics Research Letters*, Vol. 1, 255–261, 2008.

12. Wang, F. J. and J.-S. Zhang, "Wideband printed dipole antenna for multiple wireless services," *Journal of Electromagnetic Waves and Applications*, Vol. 21, No. 11, 1469–1477, 2007.

13. Mandelbrot, B. B., *The Fractal Geometry of Nature*, W. H. Freeman, New York, 1983.

14. Puente, C., J. Romeu, R. Pous, J. Pamis, and A. Hijazo, "Small but long Koch fractal monopole," *Electronics Letters*, Vol. 34, No. 1, 9–10, 1998.

15. Gianvittorio, J. P. and Y. Rahmat-Samii, "Fractal antennas: A novel antenna miniaturization technique, and applications," *IEEE Antennas Propagation Magazine*, Vol. 44, No. 1, 20–36, 2002.

16. Elkamchouchi, H. M. and M. N. A. El-Salam, "Square loop antenna miniaturization using fractal geometry," *Antenna and Propagation Society International Symposium, 2003. IEEE*, Vol. 4, 254–257, 2003.

17. Ataeiseresht, R., C. Ghobadi, and J. Nourinia, "A novel analysis of minkowski fractal microstrip patch antenna," *Journal of Electromagnetic Waves and Applications*, Vol. 20, No. 8, 1115–1127, 2006.

18. Kordzadeh, A. and F. Hodjat-Kashani, "A new reduced size microstrip patch antenna with fractal shaped defects," *Progress In Electromagnetics Research B*, Vol. 11, 29–37, 2009.

19. Puente, C., J. Romeu, R. Pous, and A. Cardama, "On the behavior of the Sierpinski multiband fractal antenna," *IEEE Transactions on Antennas and Propagation*, Vol. 46, No. 4, 517–524, 1998.

20. Romeu, J. and J. Soler, "Generalized Sierpinski fractal multiband antenna," *IEEE Transactions on Antennas and Propagation*, Vol. 49, No. 8, 1237–1239, 2001.

21. Song, C. T. P., P. S. Hall, and H. Ghafouri-Shiraz, "Multiband multiple ring monopole antennas," *IEEE Transactions on Antennas and Propagation*, Vol. 51, No. 4, 722–729, 2003.

22. Liu, J.-C., D.-C. Lou, C.-Y. Liu, C.-Y. Wu, and T.-W. Soong, "Precise determinations of the CPW-FED circular fractal slot antenna," *Microwave Opt. Technol. Lett.*, Vol. 48, No. 8, 1586–1592, 2006.

23. Congiu, S. and G. Mazzarella, "A tri-band printed antenna base on a Sierpinski gasket," *Journal of Electromagnetic Waves and Applications*, Vol. 21, No. 15, 2187–2200, 2007.

24. Mahatthanajatuphat, C. and P. Akkaraekthalin, "An NP generator model for Minkowski fractal antenna," *Proceeding of the 3rd ECTI-CON*, Vol. 2, 749–752, 2006.